The pseudo-binary mercury chalcogenide alloy $HgSe_{0.7}S_{0.3}$ at high pressure: a mechanism for the zinc blende to cinnabar reconstructive phase transition



2003 J. Phys.: Condens. Matter 15 2339

(http://iopscience.iop.org/0953-8984/15/14/310)

INSTITUTE OF PHYSICS PUBLISHING JOURNAL OF PHYSICS: CONDENSED MATTER

J. Phys.: Condens. Matter **15** (2003) 2339–2349 PII: S0953-8984(03)54601-X

# The pseudo-binary mercury chalcogenide alloy $HgSe_{0.7}S_{0.3}$ at high pressure: a mechanism for the zinc blende to cinnabar reconstructive phase transition

**D P Kozlenko[1,5], K Knorr[2], L Ehm[2], S Hull[3], B N Savenko[1], V V Shchennikov[4] and V I Voronin[4]**

[1] Frank Laboratory of Neutron Physics, JINR, 141980 Dubna Moscow Region, Russia
[2] Institut für Geowissenschaften, Mineralogie/Kristallographie, Universität Kiel, Olshausenstraße 40, D-24098 Kiel, Germany
[3] ISIS Facility, RAL, Chilton OX11 0QX, Didcot, UK
[4] Institute for Metal Physics, Ural Branch of RAS, 620219 Ekaterinburg, Russia

E-mail: denk@nf.jinr.ru

Received 30 September 2002
Published 31 March 2003
Online at stacks.iop.org/JPhysCM/15/2339

**Abstract**

The structure of the pseudo-binary mercury chalcogenide alloy $HgSe_{0.7}S_{0.3}$ has been studied by x-ray and neutron powder diffraction at pressures up to 8.5 GPa. A phase transition from the cubic zinc blende structure to the hexagonal cinnabar structure was observed at $P \sim 1$ GPa. A phenomenological model of this reconstructive phase transition based on a displacement mechanism is proposed. Analysis of the geometrical relationship between the zinc blende and the cinnabar phases has shown that the possible order parameter for the zinc blende–cinnabar structural transformation is the spontaneous strain $e_4$. This assignment agrees with the previously observed high pressure behaviour of the elastic constants of some mercury chalcogenides.

## 1. Introduction

II–VI pseudo-binary solid solutions of the $AB_{1-x}C_x$ type (A = Hg, Cd, Zn; B, C = Se, S, Te) have important applications in heterojunctions and opto-electronic devices [1]. Knowledge of the structural, transport and thermodynamic properties of these alloys is important for both manufacturing technology and the search for additional potential applications.

It has recently been shown that pseudo-binary mercury chalcogenide alloys $HgSe_{1-x}S_x$ exhibit an electronic semimetal to semiconductor phase transition under high pressure and that the transition pressure strongly depends on the sulfur content $x$ [2–4]. In a subsequent

[5] Author to whom any correspondence should be addressed.

0953-8984/03/142339+11$30.00  

structural study it has been established that $HgSe_{1-x}S_x$ alloys with $0.3 < x < 0.6$ crystallize in the cubic zinc blende structure at ambient conditions and the previously observed electronic phase transition corresponds to a structural transformation to the hexagonal cinnabar structure at $P \sim 1$ GPa [5].

Cinnabar is the ambient pressure phase of HgS (cinnabar) [6] and it has been found under high pressure in the chalcogenides HgSe [7, 8], HgTe [9–11], CdTe [12], ZnTe [13] and ZnSe [14], respectively. The role of the cinnabar phase as an intermediate structure between the fourfold coordinated zinc blende and sixfold coordinated rock salt phases in II–VI compounds has extensively been studied both experimentally [10, 11, 13, 14] and theoretically [15–18] in recent years. In the cinnabar structure (space group $P3_121$) Hg (Cd, Zn) atoms occupy sites 3(a) ($u$, 0, 1/3) and chalcogen atoms occupy sites 3(b) ($v$, 0, 5/6). Depending on the values $u$ and $v$, the structure of the cinnabar phase may exhibit different atomic arrangements with coordination numbers 2 + 4 (HgS), 4 + 2 (HgTe) and 6. The latter corresponds to the rock salt structure in its hexagonal setting, having a lattice parameter ratio $c/a = \sqrt{6}$ and $u = v = 2/3$ [10, 14].

One should note that most of the previous theoretical studies of the phase transitions in mercury chalcogenides have been based on total energy *ab initio* calculations. An alternative approach is the analysis of the symmetry changes during the phase transition and a consideration of the phenomenological model of the phase transition in the framework of Landau theory using an order parameter formalism [19, 20].

Under high pressure a decrease in the elastic constant $C_{44}$ and the elastic constant combination $\frac{1}{2}(C_{11}-C_{12})$ has been observed in HgSe and HgTe in the vicinity of the zinc blende–cinnabar phase transition [21, 22]. Consequently, a spontaneous strain of appropriate symmetry would be a primary order parameter for this phase transition.

The structure of the pseudo-binary mercury chalcogenide alloys $HgSe_{1-x}S_x$ has recently been studied [5] over a limited pressure range up to 3 GPa and no information on the pressure evolution of the cinnabar phase or other possible phase transitions has been obtained. In this work we studied the structural behaviour of the pseudo-binary alloy $HgSe_{0.7}S_{0.3}$ in the extended pressure range up to 8.5 GPa. The resultant structural data were used for the discussion of the zinc blende–cinnabar phase transition in the framework of the Landau theory for phase transitions [19, 20] and the search for a possible order parameter.

## 2. Experimental details

Polycrystalline samples of $HgSe_{0.7}S_{0.3}$ were prepared by melting high purity components HgSe and HgS (99.999%). The chemical composition of the sample was determined by means of x-ray fluorescence analysis using a 'Superprobe-JCXA-733' spectrometer. The sulfur content was determined to be 0.302(1).

X-ray powder diffraction measurements were performed at pressures up to 5 GPa with a Mar-2000 image plate diffractometer (Mo K$\alpha$ radiation, Si-(111) monochromator, $\lambda = 0.7107$ Å) using a Merrill–Bassett type diamond-anvil cell [23]. The sample was loaded in an Inconel gasket with a 4:1 methanol–ethanol mixture as a pressure transmitting medium. The pressure was measured using the ruby fluorescence technique [24]. The distance from the sample to the image plate was 102 mm and the experimental data were collected in $2\theta$ range 10°–36°. It was impossible to avoid a scattering from the gasket in experiments since a conventional x-ray tube was used. This is a divergent source and a collimation of the x-ray beam to the desirable level results in a high loss of intensity. The two-dimensional powder diffraction patterns were integrated by applying the FIT2D program [25] to give one-dimensional conventional powder diffraction profiles.

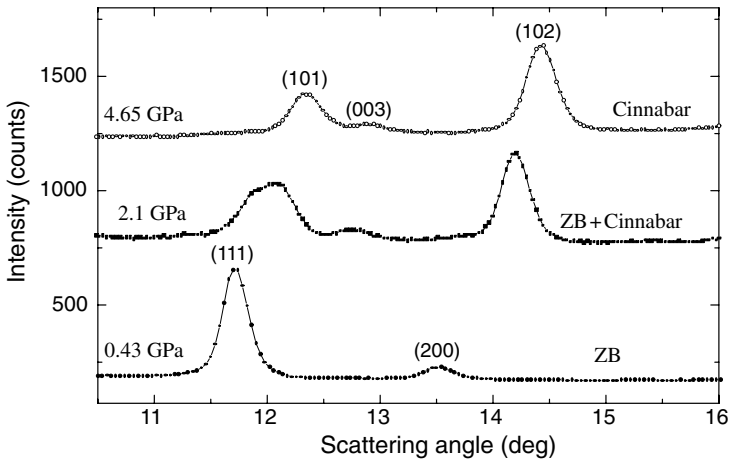


**Figure 1.** Sections of the integrated x-ray powder diffraction patterns of $HgSe_{0.7}S_{0.3}$ at pressures of 0.43, 2.1 and 4.65 GPa illustrating the evolution of the cinnabar phase with increasing pressure.

Neutron powder diffraction experiments at pressures up to 8.5 GPa were performed at the POLARIS diffractometer [26] (ISIS, RAL, UK), using the Paris–Edinburgh high pressure cell [27]. The sample of a volume $V \sim 100\,\mathrm{mm}^3$ was loaded in a gasket made from TiZr alloy. The scattering angle range was $2\theta = 84°$–$96°$ and the diffractometer resolution in this geometry is approximately $\Delta d/d \approx 0.007$. Pressures were determined using the compressibility data obtained from the x-ray diffraction measurements up to 5 GPa and their extrapolation to higher pressures. The experimental data were corrected for the effects of attenuation of the incident and scattered beams by the pressure cell components [28]. Due to the high absorption of x-rays and neutrons by the sample typical exposure times were 16–18 h for both experiments.

## 3. Results

Integrated x-ray powder diffraction patterns of $HgSe_{0.7}S_{0.3}$ obtained at three different pressures are shown in figure 1. The pattern obtained at $P = 0$ corresponds to the cubic zinc blende structure. Peaks arising from the hexagonal cinnabar phase were first observed at $P = 0.97$ GPa. The contribution from the cinnabar phase increased with pressure and the single cinnabar phase was observed at pressures above 2.1 GPa.

Refinement of the diffraction data in profile matching mode using the Fullprof program [29] provided the lattice parameters of the zinc blende and cinnabar phases as functions of pressure (table 1).

The pressure dependence of the molar volume ($V_m$) of $HgSe_{0.7}S_{0.3}$ is shown in figure 2. The zinc blende–cinnabar phase transition results in a volume discontinuity of $\Delta V_m/V_{m0} \approx 9\%$.

For the description of the compressibility of crystals, the third-order Birch–Murnaghan equation-of-state [30] is commonly used

$$P = \tfrac{3}{2}B_0(x^{-7/3} - x^{-5/3})[1 + \tfrac{3}{4}(B_1 - 4)(x^{-2/3} - 1)], \tag{1}$$

where $x = V/V_0 = V_m/V_{m0}$ is the relative volume change, $V_0$ ($V_{m0}$) is the unit cell volume (molar volume) at $P = 0$ and $B_0$ and $B_1$ are the bulk modulus and its pressure derivative. In equation (1) the pressure $P$ acts as the response variable. Since volume as well as pressure are

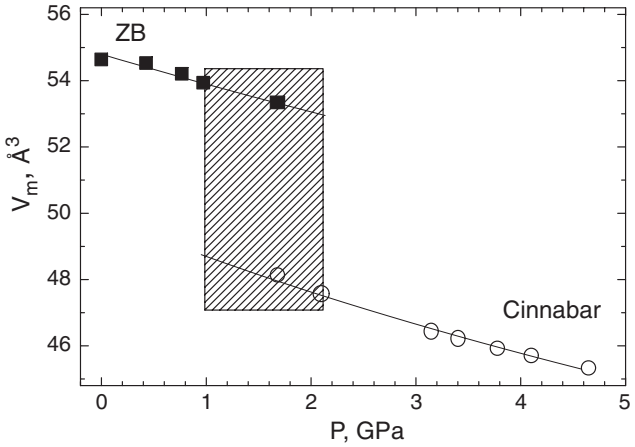


**Figure 2.** The molar volume of $HgSe_{0.7}S_{0.3}$ as a function of pressure. Error bars are within the size of the symbols. The shaded area corresponds to the region of the coexistence of the zinc blende and the cinnabar phases. The solid lines represent fits of a second-order Birch–Murnaghan equation-of-state to the experimental data.

**Table 1.** Lattice parameters of the cubic zinc blende ($a_{cub}$) and the hexagonal cinnabar ($a$, $c$) phases of $HgSe_{0.7}S_{0.3}$ as functions of pressure.

| Pressure (GPa) | $a_{cub}$ (Å) | $a$ (Å) | $c$ (Å) |
|---|---|---|---|
| 0 | 6.024(4) | — | — |
| 0.43(2) | 6.020(4) | — | — |
| 0.76(2) | 6.008(4) | — | — |
| 0.97(2) | 5.997(4) | — | — |
| 1.68(3) | 5.975(4) | 4.167(4) | 9.605(4) |
| 2.10(3) | 5.945(4) | 4.146(4) | 9.585(4) |
| 3.15(3) | — | 4.108(4) | 9.536(4) |
| 3.78(3) | — | 4.087(4) | 9.524(4) |
| 4.65(4) | — | 4.066(4) | 9.497(4) |

subject to experimental uncertainty these errors were transformed into effective variances of the pressure $\sigma_P^{\text{eff}}$ [31]:

$$\sigma_P^{\text{eff}} = \sqrt{\sigma_P^2 + (\sigma_V B_0 / V)^2}. \tag{2}$$

These effective variances were used as weights $w = 1/(\sigma_P^{\text{eff}})^2$ in the least squares refinement of the equation-of-state. As the bulk modulus $B_0$ appears in the right-hand side of equation (2) weights were re-evaluated at each iteration step of the least squares procedure. Since the compressibility data for the zinc blende and the cinnabar phases were obtained in a rather limited pressure range, it is difficult to obtain $B_0$ and $B_1$ simultaneously. Hence, values of $B_0$ and $V_{m0}$ at $P = 0$ for the zinc blende and the cinnabar phases (table 2) were obtained from the fit of the experimental data by the second-order Birch–Murnaghan equation-of-state which corresponds to equation (1) with $B_1 = 4$.

The fitted values of $B_0$ are higher than the corresponding values obtained for the binary compounds HgSe and HgS (table 2). One would expect the increase of the bulk modulus for the zinc blende phase of $HgSe_{1-x}S_x$ alloys in comparison with HgSe because partial substitution of Se atoms by S atoms decreases the average ionic radius of the X = Se/S anion. It is more

**Table 2.** The bulk modulus and molar volume at ambient pressure for the zinc blende and cinnabar phases of $HgSe_{0.7}S_{0.3}$, HgSe and HgS.

| | Zinc blende | | Cinnabar | |
|---|---|---|---|---|
| | $HgSe_{0.7}S_{0.3}$ | HgSe [21] | $HgSe_{0.7}S_{0.3}$ | HgS [9] |
| $B_0$ (GPa) | 58(7) | 51.6(2) | 39(2) | 19.4(5) |
| $B_1$ (GPa) | 4 | 2.60(6) | 4 | 11.1 |
| $V_{m0}$ (Å$^3$) | 54.8(1) | 56.3 [17] | 49.9(2) | 47.2 |

difficult to compare values of $B_0$ for the cinnabar phases of $HgSe_{1-x}S_x$ and HgS, since they exist in different pressure ranges. However, the large difference between $B_0$ for $HgSe_{1-x}S_x$ and HgS may be connected with the large value of $B_1 = 11.1$ used for a description of the compressibility data in [9]. It is well known that $B_0$ and $B_1$ are correlated parameters. Therefore it is not surprising to find smaller values for $B_0$ if $B_1$ is larger than four and vice versa. A similar situation was found for another mercury chalcogenide—HgTe [11]. For the cinnabar phase of this compound the values $B_0 = 41(10)$ GPa and $B_1 = 3.3(2)$ were obtained whilst in an earlier work a much smaller value $B_0 = 16$ GPa was obtained with $B_1 = 7.3$.

The bulk modulus $B_0$ of the cinnabar phase of $HgSe_{0.7}S_{0.3}$ is significantly lower in comparison with one for the zinc blende phase (table 2). The possible reason for this effect is an increase in the coordination number due to the zinc blende–cinnabar phase transition. There are four equal nearest-neighbour distances between Hg and Se/S atoms in the zinc blende phase and three pairs of them with a different length in the cinnabar phase [11]. The length of one pair of the nearest-neighbour distances in the cinnabar phase remains nearly the same as in the zinc blende phase but two other pairs become larger. Assuming that the main compression mechanism is a bond length shortening, one would expect a smaller value of bulk modulus for the cinnabar phase.

In addition, the pressure dependence of the lattice parameters for the cinnabar phase has been analysed. The volume in equation (1) was substituted by the cube of the lattice parameters and fitted using the second-order Birch–Murnaghan equation-of-state. The zero pressure compressibility $k_{a,c}$ is then given by $1/(3B_0)$. The compressibility along the $a$-axis is $k_a = 0.0117$ GPa$^{-1}$ and $k_c = 0.0045$ GPa$^{-1}$ along the $c$-axis. Hence, the compressibility in the cinnabar phase is anisotropic with $k_a \approx 2.6\, k_c$.

It was not possible to obtain atomic positional parameters for the cinnabar phase of $HgSe_{0.7}S_{0.3}$ from the x-ray diffraction data due to the peak overlap between the reflections of the sample and the gasket, the strong absorption by the sample and the restricted $Q$-range in the x-ray experiment. However, this information could be obtained from the neutron diffraction experiments. The neutron diffraction pattern of the cinnabar phase of $HgSe_{0.7}S_{0.3}$ measured at the POLARIS diffractometer at $P = 7.6$ GPa is shown in figure 3.

The diffraction data were refined by the Rietveld method using the program MRIA [32]. In the refinement procedure the structural model [10] in space group $P3_121$ was used, with Hg atoms occupying 3(a) sites ($u$, 0, 1/3) and X atoms (X = Se, S) occupying 3(b) sites ($v$, 0, 5/6), as found for the binary compounds HgX. The contribution to the diffraction pattern from the tungsten carbide anvils of the high pressure cell was treated as a second phase. The lattice parameters and atomic positional parameters for the cinnabar phase of $HgSe_{0.7}S_{0.3}$, the calculated nearest-neighbour interatomic distances and the obtained $R$-factors values at different pressures are given in table 3, along with the corresponding values for the binary compounds HgSe and HgS. No further phase transitions were observed in the investigated pressure range up to 8.5 GPa.

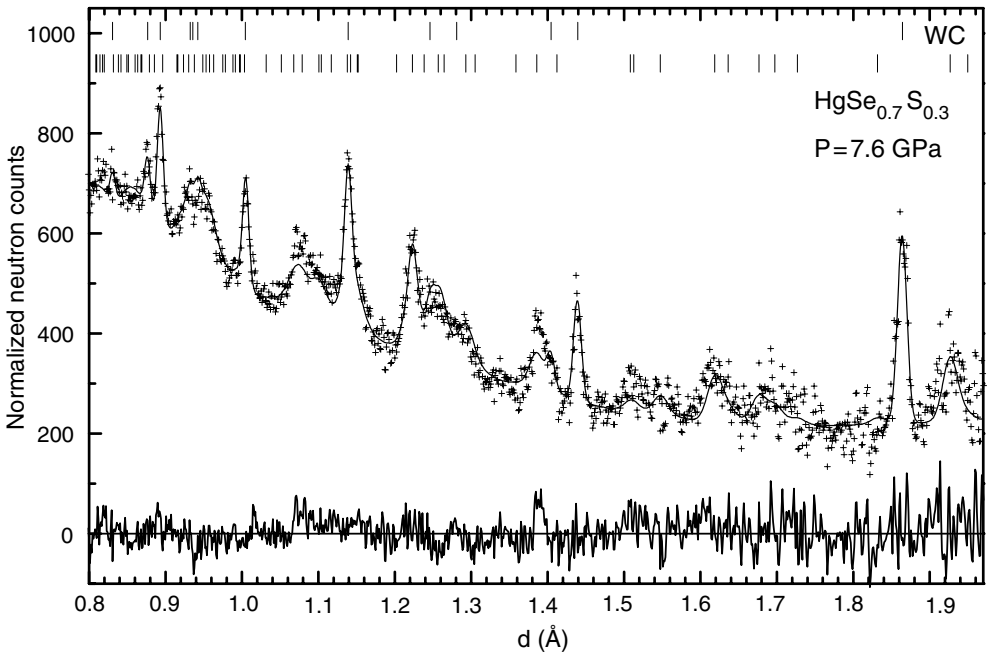


**Figure 3.** The neutron diffraction pattern of the cinnabar phase of $HgSe_{0.7}S_{0.3}$ measured at the POLARIS diffractometer at $P = 7.6$ GPa and processed by the Rietveld method. Experimental points, calculated profile and difference curve (bottom) are shown. The contribution from the tungsten carbide (WC) anvils of the high pressure cell was also included in the calculations.

**Table 3.** Refined structural parameters of the cinnabar phase of $HgSe_{0.7}S_{0.3}$ at different pressures. Lattice parameters ($a$, $c$), positional parameters of Hg and X = Se/S atoms ($u$, $v$) and the nearest-neighbour distances (Hg1–X, Hg2–X, Hg3–X) are presented. The corresponding values for the binary compounds HgSe and HgS are given for comparison.

| | $HgSe_{0.7}S_{0.3}$ | | | HgSe [8] | HgS [10] |
|---|---|---|---|---|---|
| $P$ (GPa) | 2.7(3) | 7.6(5) | 8.5(6) | 2.25 | 0 |
| $a$ (Å) | 4.127(5) | 3.982(5) | 3.957(5) | 4.174(1) | 4.14 |
| $c$ (Å) | 9.551(9) | 9.389(8) | 9.333(8) | 9.626(1) | 9.49 |
| $u$ | 0.672(7) | 0.676(7) | 0.679(7) | 0.666(1) | 0.720(3) |
| $v$ | 0.529(5) | 0.558(5) | 0.572(5) | 0.540(1) | 0.480(10) |
| Hg1–X (Å) | 2.49(2) | 2.49(2) | 2.50(2) | 2.541(4) | 2.36(5) |
| Hg2–X (Å) | 2.93(2) | 2.84(2) | 2.82(2) | 2.941(4) | 3.10(5) |
| Hg3–X (Å) | 3.28(2) | 3.08(2) | 3.01(2) | 3.299(5) | 3.30(5) |
| $R_p$ (%) | 10.7 | 10.6 | 9.0 | | |
| $R_{wp}$ (%) | 9.0 | 10.7 | 8.2 | | |

## 4. Discussion

The cinnabar structure is intermediate between the fourfold coordinated zinc blende and the sixfold coordinated NaCl-type structure [11]. The zinc blende–cinnabar phase transition is of the reconstructive type since these two structures are not related by a direct group–subgroup relationship [33].

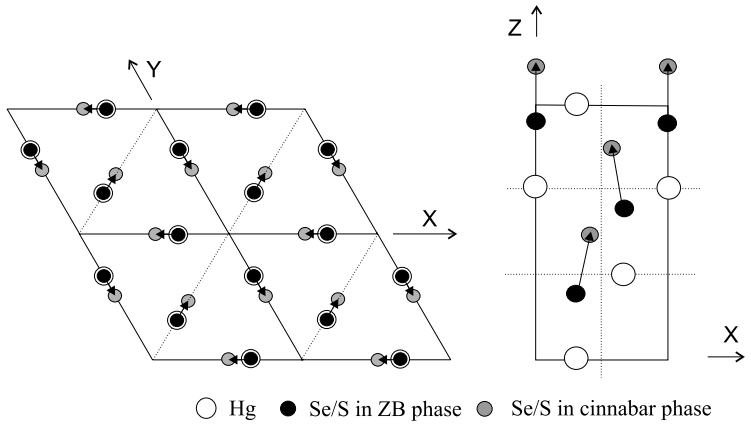


**Figure 4.** Relationship between the zinc blende structure in the hexagonal setting and the cinnabar structure. Projections of the two structures on the $XY$ plane (left) and on the $XZ$ plane (right) are shown. Displacements of the atoms due to the transition are indicated by arrows.

**Table 4.** Atomic coordinates of the zinc blende structure described in the hexagonal setting and the cinnabar structure (values of positional parameters obtained at $P = 8.5$ GPa are given).

| X = Se/S atoms | | Hg atoms | |
|---|---|---|---|
| Zinc blende—3(a) sites | Cinnabar—3(a) sites | Zinc blende—3(a) sites | Cinnabar—3(b) sites |
| (2/3, 0, 7/12) | (0.57, 0, 5/6) | (2/3, 0, 1/3) | (≈2/3, 0, 1/3) |
| (0, 2/3, 11/12) | (0.57, 0, 1/6) | (0, 2/3, 2/3) | (0, ≈2/3, 2/3) |
| (1/3, 1/3, 1/4) | (0.43, 0.43, 1/2) | (1/3, 1/3, 0) | (≈1/3, 1/3, 0) |

For the analysis of the atomic displacements at the phase transition, the zinc blende phase of $HgSe_{0.7}S_{0.3}$ may be described in a hexagonal setting (figure 4) using space group $P3_1$ with Hg and X = Se/S atoms occupying sites 3(a) $(x, y, z)$ (table 4). The characteristic feature of the zinc blende–cinnabar phase transition is a displacement of the X atoms from their initial positions 3(a) in space group $P3_1$ along the $z$-direction by $1/4c$ and along the $x$- and $y$-directions by $\varepsilon \sim 0.1\ a$ to the positions 3(b) of the space group $P3_121$. The Hg atoms remain at nearly the same positions 3(a) in both phases (tables 3, 4, figure 4).

Assuming a displacement mechanism for the transition, the transformation path from the zinc blende to the cinnabar phase can be decomposed into three successive steps:

(i) a distortion of the unit cell with the related displacement of the atoms which lowers the cubic $F\bar{4}3m$ zinc blende symmetry to $R3m$ symmetry;
(ii) a displacement of the atoms in the $z$-direction of the rhombohedral lattice which lowers further the symmetry to $R3$. This $R3$ symmetry with one molecule per unit cell can be reset in the hexagonal basis as the $P3_1$ space group with $Z = 3$;
(iii) an increase of the symmetry from $P3_1$ to $P3_121$.

This displacement mechanism is fully reversible and corresponds to Brillouin zone-centre phonon modes which involve simple deformations of the initial cubic unit cell. The assumed intermediate states display the polar symmetries $R3m$ and $R3$ (or $R3_1$), i.e. they are ferroelectric.

Among the macroscopic quantities which correspond to the symmetry breaking mechanisms at the first step of the proposed transformation path ($F\bar{4}3m \rightarrow R3m$) spontaneous

strain components $e_{yz}$, $e_{xz}$, $e_{xy}$ appear. The symmetry breaking transition from $F\bar{4}3m$ to $R3m$ is proper ferroelastic and, according to Janovec *et al* [34], the Landau condition is not fulfilled for the associated irreducible representation of the $F\bar{4}3m \rightarrow R3m$ symmetry change, i.e. a cubic term appears in the corresponding free energy expansion

$$F = \frac{\beta_0(P - P_c)}{2}Q^2 + \frac{\gamma}{3}Q^3 + \frac{\delta}{4}Q^4. \tag{3}$$

The stability condition is

$$\frac{\partial F}{\partial Q} = Q[\beta_0(P - P_c) + \gamma Q + \delta Q^2] = 0. \tag{4}$$

The order parameter $Q$ should have the symmetry of the strain. If we consider a primitive rhombohedral lattice corresponding to the zinc blende and cinnabar structures, the geometry of the displacements of the X = Se/S atoms due to the zinc blende–cinnabar phase transition allows us to assume that a spontaneous strain $e_4 = e_5 = e_6$ ($e_{yz} = e_{xz} = e_{xy}$) could be a possible order parameter.

Hence the pressure evolution of the spontaneous strain may be described as

$$e_4 = \frac{-\gamma}{2\delta}(1 + \sqrt{1 - 4\beta_0(p - p_c)\delta/\gamma^2}). \tag{5}$$

Spontaneous strain $e_4$ stems from the distortion of the lattice angle $\alpha$ of the primitive rhombohedral unit cell of the cinnabar structure in comparison with its initial value $\alpha_0 = 60^\circ$ corresponding to the cubic fcc zinc blende structure. At the first order zinc blende–cinnabar phase transition point, $e_4$ undergoes a negative jump $e_{40}$ resulting in an increasing of $\alpha$ from 60° to 62.8° and afterwards it starts to increase with a pressure increase reflecting the decrease of $\alpha$ from 62.8° to 62.1°. Figure 5 shows the square of the relative spontaneous strain ($e_4$–$e_{40}$) as a function of pressure. It increases linearly with the pressure increase, in agreement with equation (5). To estimate $e_{40}$, values of the $(a, c)$ lattice parameters of the cinnabar structure extrapolated to the estimated transition pressure $P_c = 0.97$ GPa were used and the value $e_{40} = 0.025$ was obtained.

Assuming the spontaneous strain $e_4$ to be a primary order parameter for the zinc blende–cinnabar phase transition, a softening of the elastic constant $C_{44}$ in the vicinity of the transition point should be expected [36]. In the high-pressure studies of the elastic constants of HgSe [21] and HgTe [22] a decrease in $C_{44}$ has been observed on approaching the zinc blende–cinnabar transition pressure. This is in agreement with our considerations.

The cinnabar structure is closely related to the cubic NaCl-type structure [11]. The NaCl-type structure in its hexagonal setting may be described using the same space group as for the cinnabar structure, $P3_121$, with atomic positional parameters $u = v = 2/3$. As shown in table 3, with increasing pressure the positional parameter of the Hg atoms varies slowly and remains close to its value in the zinc blende structure or the corresponding value for the NaCl-type structure, $u \sim 0.67$. The positional parameter of the X = Se/S atoms (which shifts from $v = 0.67$ to $v \sim 0.53$ at the phase transition) increases up to 0.57 in the pressure range 2.7–8.5 GPa, rending towards the value corresponding to the NaCl-type cubic structure.

There are three pairs of nearest-neighbour distances between X = Se/S and Hg atoms (Hg1–X, Hg2–X and Hg3–X) with rather close values in the cinnabar structure [10]. In $HgSe_{0.7}S_{0.3}$ the pressure increase from 2.7 to 8.5 GPa causes the shortest Hg1–X distance to remain almost constant whilst the two other distances decrease approaching the value of the first one (figure 6, table 3). This corresponds to an increase in the X–Hg–X angle (from 168.1° to 173.8°) and a decrease in the Hg–X–Hg angle from 105.4° to 99.0°. Thus, the cinnabar structure of $HgSe_{0.7}S_{0.3}$ approaches the NaCl-type cubic structure with increasing pressure,

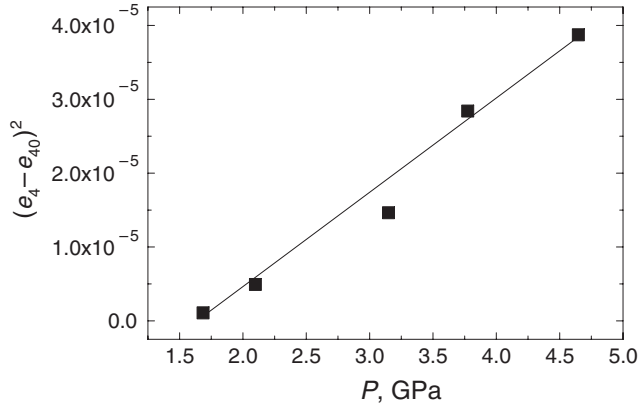


**Figure 5.** Square of the relative spontaneous strain ($e_4$–$e_{40}$) as a function of pressure. The solid line is the linear fit to the experimental data. Error bars are within the size of the symbols.

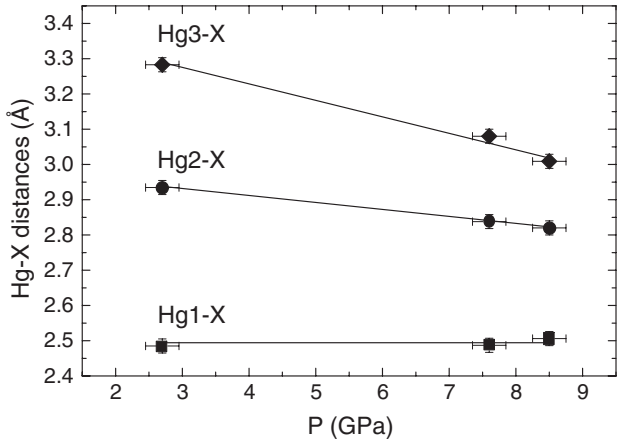


**Figure 6.** The nearest-neighbour distances between Hg and X = Se/S atoms in $HgSe_{0.7}S_{0.3}$ as functions of pressure. The solid lines are linear interpolations of the experimental data.

where the distances Hg1–X = Hg2–X = Hg3–X and the interatomic X–Hg–X and Hg–X–Hg angles have values of 180° and 90°, respectively.

A description of the coordination of the cinnabar phase of $HgSe_{0.7}S_{0.3}$ may be performed using the following ratio: $r = (l_{Hg2-X} - l_{Hg1-X})/(l_{Hg3-X} - l_{Hg2-X})$. Values of $r < 1$ correspond to a 4+2 coordination, $r > 1$ to a 2+4 coordination and $r = 1$ to the ideal sixfold coordination. The calculated value $r$ for $HgSe_{0.7}S_{0.3}$ varies from 1.26 to 1.68 as the pressure increases from 2.7 to 8.5 GPa. The increase of the distortion index $r$ shows that the difference between the Hg3–X and Hg2–X distances decreases faster than the difference between distances Hg2–X and Hg1–X on pressure increase. A comparison between $HgSe_{0.7}S_{0.3}$ and the parent binary compounds HgSe and HgS shows that the cinnabar structure of $HgSe_{0.7}S_{0.3}$ is similar to that of HgSe ($r = 1.1$, calculated from data reported in [8]) and less distorted with respect to the NaCl-type cubic structure ($r = 1$) than the cinnabar structure of HgS ($r = 3.7$) [10]. This means that the phase transition between the cinnabar and NaCl-type phases in $HgSe_{0.7}S_{0.3}$ might be expected to occur at roughly the same pressure as for HgSe, $P \sim 16$ GPa. In [38] a decrease

in the electrical resistivity by several orders of magnitude was observed in $HgSe_{0.7}S_{0.3}$ at $P \sim 15$ GPa. Such a behaviour corresponds to an electronic semiconductor–metal phase transition which accompanies the structural phase transition from the cinnabar to the NaCl-type structure in binary mercury chalcogenides HgSe, HgTe [11, 37].

## 5. Conclusions

The pressure-induced zinc blende–cinnabar phase transition has been analysed in terms of atomic displacements during the reconstructive phase transition. The proposed phenomenological model of the phase transition includes three successive steps with a symmetry change $F4\bar{3}m \rightarrow R3m \rightarrow P3_1 \rightarrow P3_121$.

The analysis of the geometry of the atomic displacements shows that a possible order parameter for the zinc blende–cinnabar structural transformation is a spontaneous strain $e_4$. This conclusion is supported by a softening of the elastic constant $C_{44}$ at this phase transition as observed in HgSe [21] and HgTe [22].

The proposed model of the zinc blende–cinnabar phase transition has a common character and may be generalized for the case of other mercury chalcogenides exhibiting this phase transition—HgSe, HgTe, CdTe, ZnTe and their pseudo-binary solutions.

The coordination and geometrical features of the cinnabar phase of $HgSe_{0.7}S_{0.3}$ are similar to those of HgSe. With increasing pressure the interatomic angles and distances of the cinnabar structure approach the values corresponding to the NaCl-type cubic structure. We therefore expect a phase transition from the hexagonal cinnabar structure to the cubic NaCl-type structure at higher pressure.

## Acknowledgments

The authors are grateful to Professor P W Toledano for the helpful discussion of the phase transition mechanism. The work was supported by the Russian Foundation for Basic Research, grants 00-02-17199 and 01-02-17203.

## References

[1] Letardi P, Motta N and Balzarotti A 1987 *J. Phys. C: Solid State Phys.* **20** 2853
[2] Shchennikov V V, Gavaleshko N P, Frasunyak V M and Osotov V I 1995 *Phys. Solid State* **37** 1311
[3] Shchennikov V V, Kar'kin A E, Gavaleshko N P and Frasunyak V M 1997 *Phys. Solid State* **39** 1528
[4] Shchennikov V V 1998 *Proc. SPIE* **3507** 254
[5] Voronin V I, Shchennikov V V, Berger I F, Glazkov V P, Kozlenko D P, Savenko B N and Tikhomirov S V 2001 *Phys. Solid State* **43** 2165
[6] Aurivillius K L 1950 *Acta Chem. Scand.* **4** 1423
[7] Mariano A N and Wareikos E P 1963 *Science* **142** 672
[8] McMahon M I, Nelmes R J, Liu H and Belmonte S A 1996 *Phys. Rev. Lett.* **77** 1781
[9] Werner A, Hochheimer H D, Strössner K and Jayaraman A 1983 *Phys. Rev.* B **28** 3330
[10] Wright N G, McMahon M I, Nelmes R J and San-Miguel A 1993 *Phys. Rev.* B **48** 13111
[11] San-Miguel A, Wright N G, McMahon M I and Nelmes R J 1995 *Phys. Rev.* B **51** 8731
[12] McMahon M I, Nelmes R J, Wright N G and Allan D R 1993 *Phys. Rev.* B **48** 16246
[13] Nelmes R J, McMahon M I, Wright N G and Allan D R 1994 *Phys. Rev. Lett.* **73** 1805
[14] Pellicer-Porres J, Segura A, Mũnoz V, Zúñiga J, Itié J P, Polian A and Munsch P 2001 *Phys. Rev.* B **65** 012109
[15] Lu Z W, Singh D and Krakauer H 1989 *Phys. Rev.* B **39** 10154
[16] Côté M, Zakharov O, Rubio A and Cohen M L 1997 *Phys. Rev.* B **55** 13025
[17] Lee G D and Ihm J 1996 *Phys. Rev.* B **53** R7622
[18] Qteish A and Mũnoz A 2001 *Phys. Status Solidi* b **223** 417
[19] Landau L D 1937 *Phys. Z. Sov. Un.* **11** 26

[20] Bruce A D and Cowley R A 1981 *Structural Phase Transitions* (London: Taylor and Francis)
[21] Ford P J, Miller A J, Saunders G A, Yoğurtçu Y K, Furdyna J K and Jaczynski M 1982 *J. Phys. C: Solid State Phys.* **15** 657
[22] Miller A J, Saunders G A, Yoğurtçu Y K and Abey A E 1981 *Phil. Mag.* **43** 1447–71
[23] Merrill L and Bassett W A 1974 *Rev. Sci. Instrum.* **45** 290
[24] Piermarini G J, Block S, Barnett J D and Forman R A 1975 *J. Appl. Phys.* **46** 2774
[25] Hammersley A P, Svensson S O, Hanfland M, Fitch A N and Häusermann D 1996 *High Press. Res.* **14** 235
[26] Hull S, Smith R I, David W I F, Hannon A C, Mayers J and Cywinski R 1992 *Physica* B **180/181** 1000
[27] Besson J M, Nelmes R J, Hamel G, Loveday J S, Weill G and Hull S 1992 *Physica* B **180/181** 907
[28] Wilson R M, Loveday J S, Nelmes R J, Klotz S and Marshall W G 1995 *Nucl. Instrum. Methods Phys. Res.* A **334** 145
[29] Rodriguez-Carvajal J 1993 *Physica* B **55** 192
[30] Birch F 1978 *J. Geophys. Res.* **83** 1257
[31] Angel R J 2000 Reviews in mineralogy and geochemistry *High-Temperature and High-Pressure Crystal Chemistry* vol 41 (Washington, DC: Mineralogical Society of America) p 35
[32] Zlokazov V B and Chernyshev V V 1992 *J. Appl. Crystallogr.* **25** 447
[33] Toledano P W and Dmitriev V P 1996 *Reconstructive Phase Transitions in Crystals and Quasicrystals* (Singapore: World Scientific)
[34] Janovec V, Dvořák V and Petzelt L 1975 *Czech. J. Phys.* **21** 1362
[35] Carpenter M A and Salje E K H 1998 *Eur. J. Mineral.* **10** 693
[36] Cowley R A 1976 *Phys. Rev.* B **13** 4877
[37] Huang T L and Ruoff A L 1985 *Phys. Rev.* B **31** 5976
[38] Shchennikov V V, Gavaleshko N P and Frasunyak V M 1993 *Phys. Solid State* **35** 199